Int J Adv Manuf Technol (2013) 64:1029–1047
DOI 10.1007/s00170-012-4071-x

ORIGINAL ARTICLE

A probabilistic approach to variation propagation control for straight build in mechanical assembly

Z. Yang · S. McWilliam · A. A. Popov · T. Hussain

Received: 14 July 2011 / Accepted: 19 March 2012 / Published online: 11 April 2012

Abstract Random component variations have a significant influence on the quality of assembled products, and variation propagation control is one of the procedures used to improve product quality in the manufacturing assembly process. This paper considers straight-build assemblies composed of axi-symmetric components and proposes a novel variation propagation control method in which individual components are re-orientated on a stage-by-stage basis to optimise the table-axis error for the final component in the assembly. Mathematical modelling methods are developed to predict the statistical variations present in the complete assembly. Three straight-build assembly strategies are considered: (a) direct build, (b) best build and (c) worst build assembly. Analytical expressions are determined for the probability density function of the table-axis error for the final component in the assembly, and comparisons are made against Monte Carlo simulations for the purposes of validation. The results show that the proposed variation propagation control method offers good accuracy and efficiency, compared to the Monte Carlo simulations. The probability density functions are used to calculate the probability that the eccentricity will exceed a particular value and are useful for industrial applications and academic research in tolerance assignment and assembly process design. The proposed method is used to analyse the influence of different component tolerances on the build quality of an example originating in aero-engine sub-assembly.

Keywords Straight-build assembly · Tolerance analysis · Monte Carlo simulation · Variation propagation control · Probabilistic approach

Z. Yang · S. McWilliam · T. Hussain
Materials, Mechanics and Structures, Faculty of Engineering,
University of Nottingham,
University Park,
Nottingham NG7 2RD, UK

Z. Yang (✉) · A. A. Popov · T. Hussain
Manufacturing Research Division, Faculty of Engineering,
University of Nottingham,
University Park,
Nottingham NG7 2RD, UK
e-mail: zhufang.yang@googlemail.com

1 Introduction

Random geometric variations from the nominal dimensions always exist in manufactured components due to imperfections in manufacturing processes. As components are assembled, these variations propagate and accumulate and can quickly drive assembly dimensions out of specification [1]. Tolerance assignment in mechanical engineering product design and manufacture is critical for product quality and cost, since the tighter tolerances needed to improve quality normally require more extensive manufacturing effort, resulting in higher manufacturing cost [2].

Improving quality and reducing the design cycle time and cost are the main objectives for competitive manufacturing today. Effectively controlling the propagation of variations in the assembly process is one way to help achieve these objectives [3]. Traditional methods for studying assembly tolerance stackup are usually based

on engineering experience, worst on worst (WOW) method [4–7], or the root-sum-square (RSS) method [2,8,9]. The WOW method often gives results that are overly pessimistic, while the RSS method only gives results for the mean-square variation. These methods are used frequently in the analysis of single-dimensional chains, and are not suited to the analysis of geometric tolerances [2,10]. Furthermore, these methods do not take into account practical assembly procedures and can be difficult to use in practice. There is a clear need to take account of random component variability during assembly to determine the likelihood that the mechanical assembly is acceptable or not.

The simplest and most popular method for statistical tolerance analysis is the Monte Carlo simulation method. Random dimensions for each component are generated according to known or assumed statistical distributions, and the relevant key characteristic (e.g. eccentricity) is computed for each set of component values. In this way, sample response function values are generated and the probability calculated that the key characteristic is satisfied or not. The main drawback of this method is that it is necessary to generate a large number of samples to achieve accurate predictions [11–14], which may require intensive computation. This issue is particularly apparent if a tolerance analysis is carried out within an iterative loop of the more complex tolerance synthesis problem. In this situation, the solution can become extremely time consuming and computationally expensive.

This paper considers the special case of mechanical assemblies composed of axi-symmetric (or polyhedral) components [15–20]. These assemblies are used in aero-engines [21] (see Fig. 1) and in gas turbines and possess the special property that the assembly can be modified by rotating components relative to each other about the central axis of symmetry. This property offers the possibility of improving assembly quality by choosing the most suitable orientations of components, and in this work, component orientations are selected at each stage of assembly to help achieve straight build. Connective assembly models are used to describe the assembly process mathematically, and a probabilistic approach is used to predict the probability that the eccentricity of the final component in the assembly is within specified threshold values. Initially the aim is to predict the probability density function (pdf) for the eccentricity of the final component, avoiding the need to use Monte Carlo simulation. Once the pdf has been constructed, the probability that the eccentricity does not exceed a particular threshold value is calculated. The main challenge in the work is to determine the pdf for the eccentricity. The main reason for this is that the connective assembly models used to describe the assembly are often complex and non-linear (see [22]), particularly when the orientation of each component is manually selected to control variation propagation. This complication is handled by adopting the practical approximation that real component variations are small compared to their nominal values [22–24], allowing the connective assembly models to be linearised and the pdfs to be obtained more easily. A simplified version of the approach is applied to two-dimensional assemblies in (Yang et al., submitted for publication)

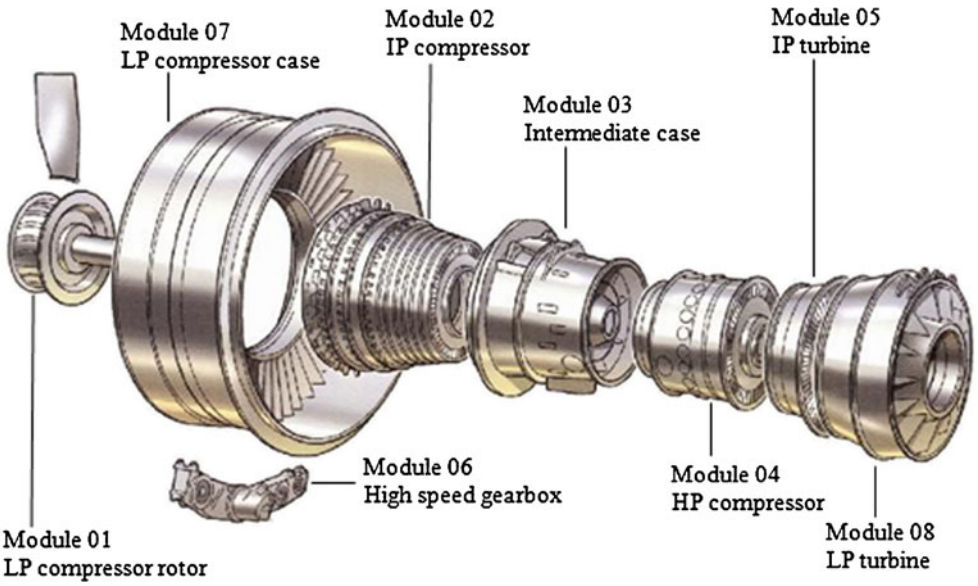

Fig. 1 The modular breakdown of a Trent family engine [21]

to illustrate some of the basic concepts for the purposes of visualisation but is limited in its application compared to the practical fully three-dimensional case considered here.

Three different straight-build strategies are considered here: (a) direct build, (b) best build and (c) worst build assembly. Direct build assembly (DBA) corresponds to the standard straight-build process in which axi-symmetric components are assembled without giving any consideration to controlling the eccentricity of the build. Best build assembly (BBA) takes advantage of the axi-symmetric property of the components and aims to minimise the eccentricity of the final component in the build. This is achieved by rotating the component being added at each stage about its nominal axis of symmetry. Worst build assembly (WBA) is the antithesis of BBA and rotates each component as it is added so as to maximise the eccentricity. Whilst WBA has no practical significance, it is useful for the purposes of comparison, and both BBA and WBA are useful in the tolerance synthesis problem.

In what follows, connective assembly models are developed in Section 2 to describe the assembly processes using the different straight-build strategies. Linearised models are used to determine the pdf for the eccentricity of the final component in an axi-symmetric assembly, using DBA, BBA and WBA in Section 3. The pdf is then used to calculate the probability that the eccentricity does not exceed a particular threshold value. In Section 4, numerical examples are presented to validate the proposed methods and investigate the influence of using different tolerances on the eccentricity of an example originating in aero-engine sub-assembly. Some practical considerations and discussions are given in Section 5.

2 Modelling straight build for an axi-symmetric assembly

Straight-build assembly is the process of assembling axi-symmetric rigid components so as to achieve an axi-symmetric build. Due to the presence of manufacturing variations, neither the components nor the assembly are perfectly axi-symmetric, and it is often necessary to monitor and control the buildup of assembly errors. In this work, the eccentricity of the final component in the complete assembly is used as a measure of the quality of the build.

Figure 2 shows a two-component axi-symmetric assembly with the upper component shown in two different orientations. Figure 2a shows the upper component in its original orientation, whilst Fig. 2b shows the upper component rotated about its axis of symmetry. The eccentricity of each build is defined by the so-called table-axis error, which is the perpendicular distance of the centre of the uppermost component (C2) from the so-called table axis, which is defined by a line that passes through the centre of the base of the first component and is perpendicular to it. For the case shown, it is clear that the configuration shown in Fig. 2b has a smaller table-axis error than that shown in Fig. 2a. By selecting the orientation of the upper component that minimises the table-axis error, the quality of the build can be improved and the "best build" achieved. In later sections, the component being added at a particular stage is rotated so that the eccentricity of the final component in the complete assembly is minimised.

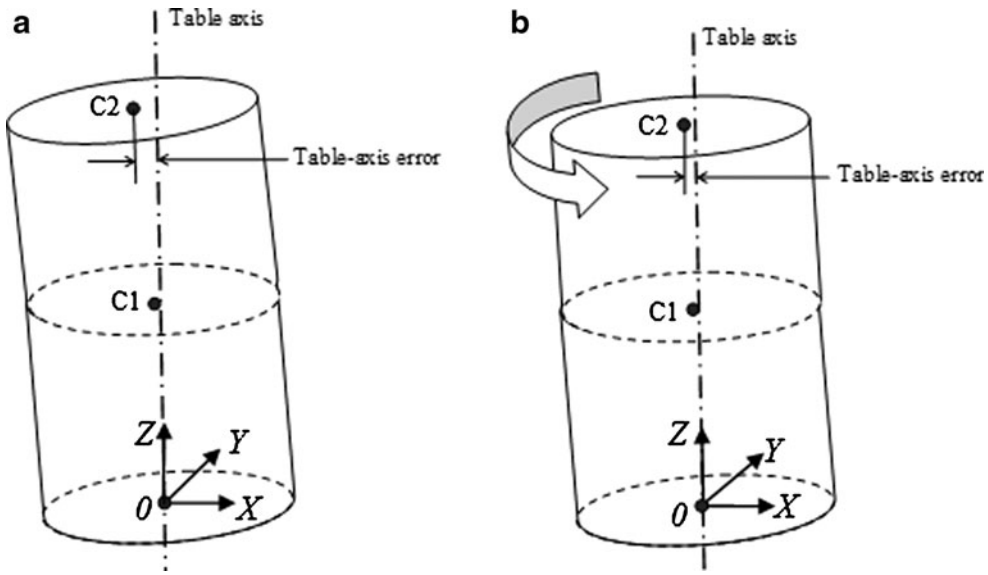

Fig. 2 Straight-build assembly: **a** original configuration and **b** after the upper component has been re-orientated to minimise the table-axis error

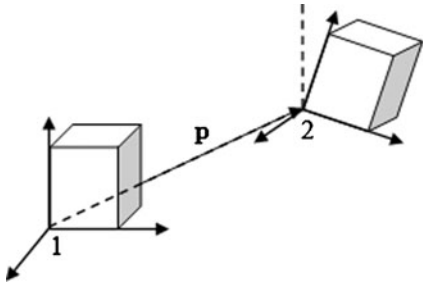

Fig. 3 Geometric relationship between two coordinate frames [22]

Mathematical models are used to predict the location and orientation of components in the assembly. In what follows, a connective assembly model is presented and applied to nominally axi-symmetric components and assemblies, and a linearised form of equations is derived when the dimensional variations are small. The linearisation allows analytical expressions to be obtained for the eccentricity (table-axis error), which are used as the starting point for the probabilistic analysis considered in Section 3. Section 2.1 provides a review of connective assembly models, and Section 2.2 presents the linearised model.

2.1 Connective assembly models for straight-build assembly

Connective assembly models [22] are used to quantify the propagation of component variations through the assembly. In these models, matrix transformations are used to relate the location and orientation of different features on one component to another component, and for this purpose, coordinate frames are attached to each of the mating features on each component. For three-dimensional components, the geometric relationship between any two coordinate frames is depicted as shown in Fig. 3.

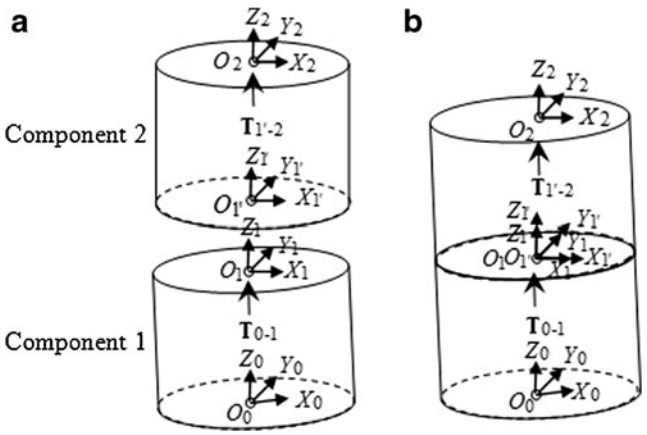

Fig. 4 An example two-component assembly: **a** unassembled and **b** assembled

In Fig. 3, the geometric relationship between coordinate frame 1 and coordinate frame 2 is represented using transformation matrix **T**. The transformation matrix represents the operations of translation and rotation acting on a coordinate frame originally aligned with a reference coordinate frame [22] and is given by:

$$T = \begin{bmatrix} R & p \\ 0^T & 1 \end{bmatrix}, \tag{1}$$

where **R** is a 3×3 rotational matrix indicating the orientation of frame 2 relative to frame 1, **p** is a 3×1 displacement vector indicating the position of frame 2 relative to frame 1 and superscript T indicates a vector or matrix transpose.

For a two-component assembly, as shown in Fig. 4, the model assumes the components are joined to each other by mating features [22] and transformation matrices are used to relate the location of the mating features, where no manufacturing variations are present. For the assembly shown in Fig. 4b, the transform matrix T^N_{0-2} relating the location and orientation of the coordinate frame at the top of component 2 to the coordinate frame at the base of component 1 can be expressed as follows:

$$\mathrm{T}^N_{0-2} = \mathrm{T}^N_{0-1}\,\mathrm{T}^N_{1-1'}\,\mathrm{T}^N_{1'-2}, \tag{2}$$

where $\mathrm{T}^N_{1-1'}$ is the transform matrix relating the location and orientation of the coordinate frame at mating feature 1′ on component 2 to the coordinate frame at mating feature 1 on component 1; $\mathbf{T}^N_{0-1}$ and $\mathbf{T}^N_{1'-2}$ are the transformation matrices relating features 0 and 1 on nominal component 1 and features 1′ and 2 on nominal component 2, respectively. Transformations $\mathrm{T}^N_{1-1'}$, $\mathbf{T}^N_{0-1}$ and $T^N_{1'-2}$ have the same form as Eq. (1). The superscript N indicates that the transform matrices relate to the nominal geometry of the component and ensures there is perfect alignment between mating features. For nominal axi-symmetric components, the upper and lower surfaces are parallel to each other and the axes for each coordinate frame are aligned perfectly. This ensures that the rotational matrix **R** (see Eq. (1)), defining the relative orientation between coordinate frames, is the identity matrix and the position vector **p** (see Eq. (1)), defining the relative location between the origins of the mating coordinate frames, is a zero vector, except in the vertical Z-direction. Using these

definitions, the transformation on the right-hand side of Eq. (2) can be expressed as:

$$\mathbf{T}_{0-1}^{N} = \begin{bmatrix} \mathbf{I} & \mathbf{p}_1^N \\ \mathbf{0}^T & 1 \end{bmatrix}, \tag{3}$$

$$\mathbf{T}_{1'-2}^{N} = \begin{bmatrix} \mathbf{I} & \mathbf{p}_2^N \\ \mathbf{0}^T & 1 \end{bmatrix}, \tag{4}$$

$$\mathbf{T}_{1-1'}^{N} = \begin{bmatrix} \mathbf{I} & \mathbf{0} \\ \mathbf{0}^T & 1 \end{bmatrix}, \tag{5}$$

$$\mathbf{p}_i^N = \begin{bmatrix} 0 \\ 0 \\ Z_i \end{bmatrix}, \tag{6}$$

where Z_i is the height of the ith component and i=1,2. Using these equations in Eq. (2) gives:

$$\mathbf{T}_{0-2}^{N} = \begin{bmatrix} \mathbf{I} & \mathbf{p}_1^N + \mathbf{p}_2^N \\ \mathbf{0}^T & 1 \end{bmatrix}. \tag{7}$$

In a similar way, the transform matrix for an assembly consisting of n axi-symmetric components can be expressed as:

$$\mathbf{T}_{0-n}^{N} = \begin{bmatrix} \mathbf{I} & \sum_{i=1}^{n} \mathbf{p}_i^N \\ \mathbf{0}^T & 1 \end{bmatrix}, \tag{8}$$

where $\mathbf{T}_{0-n}^{N}$ is the transform matrix relating the location and orientation of the coordinate frame at the top of component n to the coordinate frame at the base of component 1.

If a feature on a part is not placed at its nominal design position due to manufacturing variations, relative rotation and location errors need to be included in the definition of the relevant matrix transforms. This is achieved by introducing a matrix transform $\mathbf{D}$, having the same form as Eq. (1), for each matrix transform between two mating features on the same part. Transform matrix $\mathbf{T}_{0-2}$ relating frame 2 to frame 0 can then be expressed as:

$$\mathbf{T}_{0-2} = \mathbf{T}_{0-1}^{N}\, \mathbf{D}_1\, \mathbf{T}_{1'-2}^{N}\, \mathbf{D}_2, \tag{9}$$

where $\mathbf{T}_{0-1}^{N}$ and $\mathbf{T}_{1'-2}^{N}$ are given by Eqs. (3) and (4), respectively, and transform matrix $\mathbf{D}_i$ takes account of manufacturing variations in component i, is:

$$\mathbf{D}_i = \begin{bmatrix} \mathbf{dR}_i & \mathbf{dp}_i \\ \mathbf{0}^T & 1 \end{bmatrix}, \tag{10}$$

$$\mathbf{dp}_i = \begin{bmatrix} dX_i \\ dY_i \\ dZ_i \end{bmatrix}. \tag{11}$$

The translation error vector $\mathbf{dp}_i$ takes account of translation errors $\mathrm{d}X_i$, $\mathrm{d}Y_i$ and $\mathrm{d}Z_i$ in the X-, Y- and Z-directions, respectively. The rotation error matrix $\mathbf{dR}_i$ accounts for rotation errors $\mathrm{d}\theta_{Xi}$, $\mathrm{d}\theta_{Yi}$, $\mathrm{d}\theta_{Zi}$ about the X-, Y- and Z-axes, respectively, and is formed by considering the rotation error matrices for each of these rotations and then combining them together. The rotation error matrices for the individual rotations about the X-, Y- and Z-directions are expressed as $\mathbf{dR}_{\theta Xi}$, $\mathbf{dR}_{\theta Yi}$ and $\mathbf{dR}_{\theta Zi}$, respectively, and are given in [22].

The combined rotation error matrix $\mathbf{dR}_i$ is created by multiplying matrices $\mathbf{dR}_{\theta Xi}$, $\mathbf{dR}_{\theta Yi}$ and $\mathbf{dR}_{\theta Zi}$ together (in order) and is given by:

$$\mathbf{dR}_i = \begin{bmatrix} \cos(\mathrm{d}\theta_{Yi})\cos(\mathrm{d}\theta_{Zi}) & -\cos(\mathrm{d}\theta_{Yi})\sin(\mathrm{d}\theta_{Zi}) & \sin(\mathrm{d}\theta_{Yi}) \\ \sin(\mathrm{d}\theta_{Xi})\sin(\mathrm{d}\theta_{Yi})\cos(\mathrm{d}\theta_{Zi}) & \cos(\mathrm{d}\theta_{Xi})\cos(\mathrm{d}\theta_{Zi}) & -\sin(\mathrm{d}\theta_{Xi})\cos(\mathrm{d}\theta_{Yi}) \\ +\cos(\mathrm{d}\theta_{xi})\sin(\mathrm{d}\theta_{zi}) & -\sin(\mathrm{d}\theta_{Xi})\sin(\mathrm{d}\theta_{Yi})\sin(\mathrm{d}\theta_{Zi}) & \\ \sin(\mathrm{d}\theta_{Xi})\sin(\mathrm{d}\theta_{Zi}) & \cos(\mathrm{d}\theta_{Xi})\sin(\mathrm{d}\theta_{Yi})\sin(\mathrm{d}\theta_{Zi}) & \cos(\mathrm{d}\theta_{Xi})\cos(\mathrm{d}\theta_{Yi}) \\ -\cos(\mathrm{d}\theta_{Xi})\sin(\mathrm{d}\theta_{Yi})\cos(\mathrm{d}\theta_{Zi}) & +\sin(\mathrm{d}\theta_{Xi})\cos(\mathrm{d}\theta_{Zi}) & \end{bmatrix} \tag{12}$$

In Fig. 4, if components 1 and 2 are assembled together and component 2 is rotated by an angle θ_{Z2} about the Z-axis, then transformation matrix $\mathbf{T}_{1-1'}$ must take account of this rotation. In this case, the transformation matrix $\mathbf{T}_{0-2}$ between feature 0 on component 1 and feature 2 on component 2, taking into account manufacturing variations can be written as:

$$\mathbf{T}_{0-2} = \mathbf{T}_{0-1}^{N}\, \mathbf{D}_1\, \mathbf{T}_{1-1'}\, \mathbf{T}_{1'-2}^{N}\, \mathbf{D}_2\,. \tag{13}$$

where

$$\mathbf{T}_{1-1} = \begin{bmatrix} \mathbf{S}_2 & \mathbf{0} \\ \mathbf{0}^T & 1 \end{bmatrix}, \tag{14}$$

$$\mathbf{S}_2 = \begin{bmatrix} \cos(\theta_{Z2}) & -\sin(\theta_{Z2}) & 0 \\ \sin(\theta_{Z2}) & \cos(\theta_{Z2}) & 0 \\ 0 & 0 & 1 \end{bmatrix}, \tag{15}$$

and $\mathbf{s}_2$ is the rotation matrix that takes account of rotating component 2 by an angle θ_{Z2} about the Z-axis to control the resulting eccentricity.

Using Eqs. (3), (4), (6), (10), (11), (14) and (15) in Eq. (13), $\mathbf{T}_{0-2}$ can be expressed as:

$$T_{0-2} = \begin{bmatrix} \mathbf{dR}_1\mathbf{S}_2\mathbf{dR}_2 & \left(\mathbf{p}_1^N + \mathbf{dp}_1\right) + \mathbf{dR}_1\mathbf{S}_2\left(\mathbf{p}_2^N + \mathbf{dp}_2\right) \\ \mathbf{0}^T & 1 \end{bmatrix}. \tag{16}$$

For an n-component assembly, it can be shown that the transformation matrix $\mathbf{T}_{0-n}$ is given by:

$$\mathbf{T}_{0-n} = \begin{bmatrix} \prod_{i=1}^{n}\left(\mathbf{S}_i\mathbf{dR}_i\right) & \sum_{i=1}^{n}\left(\prod_{i=2}^{n}\mathbf{S}_{j-1}\mathbf{dR}_{j-1}\right)S_i\left(\mathbf{p}_i^N + \mathbf{dp}_i\right) \\ 0^T & 1 \end{bmatrix}, \tag{17}$$

Equation (17) can be used to determine the rotation and translation errors for the nth component in an assembly and forms the basis for calculating the table-axis error for the complete assembly.

2.2 Linearised straight-build assembly models

In practical applications, component geometric variations are small compared to the nominal values and taking this into account greatly simplifies Eq. (17). In what follows, the translation errors $\mathrm{d}X_i$, $\mathrm{d}Y_i$, $\mathrm{d}Z_i$ and rotation angle errors $\mathrm{d}\theta_{Xi}$, $\mathrm{d}\theta_{Yi}$, $\mathrm{d}\theta_{Zi}$ are assumed to be small, and a simplified version of Eq. (17) is obtained.

Assuming that the rotation angle errors are small, Eq. (12) can be approximated as follows:

$$\mathbf{dR}_i = \mathbf{I} + \delta\mathbf{R}_i, \tag{18}$$

where

$$\delta\mathbf{R}_i = \begin{bmatrix} 0 & -\mathrm{d}\theta_{Zi} & \mathrm{d}\theta_{Yi} \\ \mathrm{d}\theta_{Zi} & 0 & -\mathrm{d}\theta_{Xi} \\ -\mathrm{d}\theta_{Yi} & \mathrm{d}\theta_{Xi} & 0 \end{bmatrix}, \tag{19}$$

and first-order small-angle approximations have been used such that $\cos(\mathrm{d}\theta)\approx 1$, $\sin(\mathrm{d}\theta)\approx\mathrm{d}\theta$. Using Eqs. (6) and (15), it can be shown that $\mathbf{S}_i\,\mathbf{p}_i^N = \mathbf{p}_i^N$. In accordance with these approximations, second- and higher-order products of $\boldsymbol{\delta}\mathbf{R}_i$ and $\mathbf{dp}_j$ are assumed to be negligibly small, and Eq. (17) can be approximated as follows:

$$\mathbf{T}_{0-n}^{\mathrm{Approx}} = \begin{bmatrix} \prod_{i=1}^{n}\mathbf{S}_i + \sum_{i=1}^{n}\left(\left(\prod_{j=1}^{i}\mathbf{S}_j\right)\delta\mathbf{R}_i\left(\prod_{k=i+1}^{n}\mathbf{S}_k\right)\right)\sum_{i=1}^{n}\mathbf{p}_i^N + \sum_{i=1}^{n-1}\left(\prod_{j=1}^{i}\mathbf{S}_j\right)\left(\mathbf{dp}_i + \delta\mathbf{R}_i\left(\sum_{k=i+1}^{n}\mathbf{p}_k^N\right)\right) + \left(\prod_{i=1}^{n}\mathbf{S}_i\right)\mathbf{dp}_n \\ \mathbf{0}^T\,1 \end{bmatrix} \tag{20}$$

Comparing Eqs. (20) and (8), the translation error vector for the mating feature located on the upper surface of the nth component is given by:

$$\begin{bmatrix} \mathrm{d}x_n \\ \mathrm{d}y_n \\ \mathrm{d}z_n \end{bmatrix} = \sum_{i=1}^{n-1}\left(\prod_{j=1}^{i}\mathbf{S}_j\right)\left(\mathbf{dp}_i + \delta\mathbf{R}_i\left(\sum_{k=i+1}^{n}\mathbf{p}_k^N\right)\right) + \left(\prod_{i=1}^{n}\mathbf{S}_i\mathbf{dp}_n\right). \tag{21}$$

where $\mathrm{d}x_n$ and $\mathrm{d}y_n$ define the table-axis error and $\mathrm{d}z_n$ is the vertical height error for the nth component in the assembly.

Equation (21) is used as a basis for determining an expression for vector $[\mathrm{d}x_n, \mathrm{d}y_n]$, which is needed to determine the eccentricity of the nth component in the assembly. Using Eqs. (6), (11), (15) and (19) in Eq. (21), it can be shown that:

$$\begin{bmatrix} \mathrm{d}x_n \\ \mathrm{d}y_n \end{bmatrix} = \sum_{j=1}^{n} r_j^{(n)}\begin{bmatrix} \cos\left(\alpha_j + \beta_j^{(n)}\right) \\ \sin\left(\alpha_j + \beta_j^{(n)}\right) \end{bmatrix}. \tag{22}$$

This equation is used later to determine an explicit expression for the eccentricity using direct build assembly, worst build assembly and best build assembly.where

$$\alpha_j = \sum_{k=1}^{j}\theta_{Zk},$$

$$r_j^{(n)} = \sqrt{\left(\mathrm{d}X_j + \mathrm{d}\theta_{Yj}\left(\sum_{k=j+1}^{n}Z_k\right)\right)^2 + \left(\mathrm{d}Y_j - \mathrm{d}\theta_{Xj}\left(\sum_{k=j+1}^{n}Z_k\right)\right)^2}, \tag{23}$$

$$\tan\beta_j^{(n)} = \frac{\mathrm{d}Y_j - \mathrm{d}\theta_{Xj}\left(\sum_{k=j+1}^{n}Z_k\right)}{\mathrm{d}X_j + \mathrm{d}\theta_{Yj}\left(\sum_{k=j+1}^{n}Z_k\right)}, \tag{24}$$

for j=1,2,..,(n−1), and

$$r_n^{(n)} = \sqrt{\mathrm{d}X_n^2 + \mathrm{d}Y_n^2} \tag{25}$$

$$\tan\beta_n^{(n)} = \frac{\mathrm{d}Y_n}{\mathrm{d}X_n} \tag{26}$$

In these equations, superscript (n) indicates that the quantity refers to the nth component in the assembly.

Using complex notation and Eq. (22), the eccentricity of the nth component in the assembly ε_n can be written as:

$$\varepsilon_n = \left|\sum_{j=1}^{n} r_j^{(n)} \exp\left(i\gamma_j^{(n)}\right)\right|, \tag{27}$$

where $\gamma_j^{(n)} = \alpha_j + \beta_j^{(n)}$. The jth term in the summation on the right side of Eq. (27) denotes the contribution arising from manufacturing variations in, and rotation of, the jth component to the eccentricity of the nth component and can be interpreted as a vector of length $r_j^{(n)}$ and orientation $\gamma_j^{(n)}$. It is worth noting that length $r_j^{(n)}$ depends on translational ($\mathrm{d}X_j$, $\mathrm{d}Y_j$) and rotational ($\mathrm{d}\theta_{Xj}$, $\mathrm{d}\theta_{Yj}$) variations for the jth component only, whilst orientation $\gamma_j^{(n)}$ depends on the rotations (θ_{Zj}) applied to the first j components and rotational variation $\left(\beta_j^{(n)}\right)$ for the jth component. When applying the worst build assembly and best build assembly strategies, each component is rotated to maximise or minimise the eccentricity, respectively. As each $\gamma_j^{(n)}$ contains an additional rotation (θ_{Zj}) compared to $\gamma_{j-1}^{(n)}$, each orientation γ_j can be considered to be completely independent of all other orientations $\gamma_k^{(n)}$ ($k \neq j$).

2.2.1 Direct build assembly

For direct build assembly, no attempt is made to control the propagation of component variations as the assembly is built. Setting α_j=0 in Eq. (22) and using the resulting equation, it can be shown easily that the eccentricity $\varepsilon_n^{\mathrm{Direct}}$ for the nth component in the assembly is given by:

$$\varepsilon_n^{\mathrm{Direct}} = \sqrt{\left(\sum_{i=1}^{n}\mathrm{d}X_i + \sum_{i=1}^{n-1}\mathrm{d}\theta_{Yi}\sum_{j=i+1}^{n}Z_j\right)^2 + \left(\sum_{i=1}^{n}\mathrm{d}Y_i - \sum_{i=1}^{n-1}\mathrm{d}\theta_{Xi}\sum_{j=i+1}^{n}Z_j\right)^2}. \tag{28}$$

2.2.2 Worst build assembly

For worst build assembly, the build eccentricity is maximised by rotating each component about its axis of symmetry and selecting the assembly configuration that provides the maximum eccentricity for the final component in the assembly. The WBA eccentricities for n=2, n=3 and the general case of an n-component assembly are considered below.

For a two-component assembly (n=2), the maximum eccentricity is obtained by selecting the orientation angle θ_{Z2} for component 2 such that: $\gamma_2^{(2)} = \gamma_1^{(2)}$ (i.e. $\theta_{Z2} = \beta_1^{(2)} - \beta_2^{(2)}$). This ensures the vectors defining the eccentricity are collinear and act in the same "outwards" direction. Applying this procedure and using Eqs. (23)–(25) and (27), the maximum eccentricity is given by:

$$\varepsilon_2^{\max} = \max_{\theta_{Z2}}\left|r_1^{(2)}\exp\left(i\gamma_1^{(2)}\right) + r_2^{(2)}\exp\left(i\gamma_2^{(2)}\right)\right| = \sum_{i=1}^{2} r_i^{(2)} = \sqrt{(\mathrm{d}X_1 + \mathrm{d}\theta_{Y1}Z_2)^2 + (\mathrm{d}Y_1 - \mathrm{d}\theta_{X1}Z_2)^2} + \sqrt{\mathrm{d}X_2^2 + \mathrm{d}Y_2^2}. \tag{29}$$

For a three-component assembly (n=3), the maximum eccentricity is achieved by selecting orientation angles θ_{Z2} and θ_{Z3} for components 2 and 3, respectively, such that $\gamma_2^{(3)} = \gamma_1^{(3)}$ (i.e. $\theta_{Z2} = \beta_1^{(3)} - \beta_2^{(3)}$) and $\gamma_3^{(3)} = \gamma_1^{(3)}$ (i.e. $\theta_{Z3} = \beta_2^{(3)} - \beta_3^{(3)}$). This is equivalent to the vectors defining the eccentricity being collinear with all components acting in the same "outwards" sense. Applying this procedure and using Eqs. (23)–(25)

and (27), the maximum eccentricity is given by:

$$\begin{aligned}\varepsilon_3^{\max} &= \max_{\theta_{Z2},\theta_{Z3}} \left| r_1^{(3)} \exp\left(i\gamma_1^{(3)}\right) + r_2^{(3)} \exp\left(i\gamma_2^{(3)}\right) + r_3^{(3)} \exp\left(i\gamma_3^{(3)}\right) \right| = \sum_{i=1}^{3} r_i^{(3)} \\ &= \sqrt{\left(\mathrm{d}X_1 + \mathrm{d}\theta_{Y1}(Z_2+Z_3)\right)^2 + \left(\mathrm{d}Y_1 - \mathrm{d}\theta_{X1}(Z_2+Z_3)\right)^2} \\ &\quad + \sqrt{\left(\mathrm{d}X_2 + \mathrm{d}\theta_{Y2}Z_3\right)^2 + \left(\mathrm{d}Y_2 - \mathrm{d}\theta_{X2}Z_3\right)^2} + \sqrt{\mathrm{d}X_3^2 + \mathrm{d}Y_3^2}.\end{aligned} \tag{30}$$

For an n-component assembly, the maximum eccentricity can be obtained in an identical way and is given by:

$$\varepsilon_n^{\max} = \max_{\theta_{Z2},\theta_{Z3},\ldots,\theta_{Zn}} \left| \sum_{j=1}^{n} r_j^{(n)} \exp\left(i\gamma_j^{(n)}\right) \right| = \sum_{i=1}^{n} r_i^{(n)} = \sum_{i=1}^{n-1} \sqrt{\left(\mathrm{d}X_i + \mathrm{d}\theta_{Yi} \sum_{j=i+1}^{n} Z_j\right)^2 + \left(\mathrm{d}Y_i - \mathrm{d}\theta_{Xi} \sum_{j=i+1}^{n} Z_j\right)^2} + \sqrt{\mathrm{d}X_n^2 + \mathrm{d}Y_n^2}. \tag{31}$$

In the practical assembly process, components are assembled stage by stage, and at each of these stages, the orientation of the upper most component (only) is modified to control the eccentricity. Since WBA is independent of the order in which the components are re-orientated, this stage-by-stage assembly yields the maximum eccentricity.

2.2.3 Best build assembly

For best build assembly, the build eccentricity is minimised by rotating each component about its axis of symmetry and selecting the assembly configuration that provides the minimum eccentricity for the final component. In contrast to WBA, it is more difficult to determine the assembly configuration having minimum eccentricity for assemblies with three or more components, and for this reason, an approximate approach will be developed that is well suited to the stage-by-stage assembly process. The BBA eccentricities for n=2, n=3 and the general case of an n-component assembly are considered below.

For a two-component assembly (n=2), the minimum eccentricity is obtained by selecting the orientation angle θ_{Z2} for component 2 such that: $\gamma_2^{(2)} = \gamma_1^{(2)} + \pi$ (i.e. $\theta_{Z2} = \beta_1^{(2)} - \beta_2^{(2)} + \pi$). This ensures the two vectors defining the eccentricity are collinear, but act in the *opposite* sense. Applying this procedure and using Eqs. (23)–(25) and (27), the minimum eccentricity is given by:

$$\varepsilon_2^{\min} = \min_{\theta_{Z2}} \left| r_1^{(2)} \exp\left(i\gamma_1^{(2)}\right) + r_2^{(2)} \exp\left(i\gamma_2^{(2)}\right) \right| = \left| r_1^{(2)} - r_2^{(2)} \right| = \left| \sqrt{\left(\mathrm{d}X_1 + \mathrm{d}\theta_{Y1}Z_2\right)^2 + \left(\mathrm{d}Y_1 - \mathrm{d}\theta_{X1}Z_2\right)^2} - \sqrt{\mathrm{d}X_2^2 + \mathrm{d}Y_2^2} \right|. \tag{32}$$

For a three-component assembly (n=3), the minimum eccentricity is obtained by selecting orientation angles θ_{Zk} (k=2,3) to minimise Eq. (27). Unlike WBA, BBA for assemblies with three or more components requires the resultant eccentricity vector to be minimised and does not necessarily coincide with the individual eccentricity vectors being collinear. In these situations, it is necessary to perform a full optimisation to achieve the minimum, and it is not possible to write simple analytical expressions. In what follows, an approximate expression for the minimum eccentricity is derived based on the assumption that the eccentricity vectors are collinear. For a three-component assembly, this is achieved in two steps. The first step is to select the orientation of

component 2 to minimise the eccentricity for the final (third) component based on variations in components 1 and 2 only, with component 3 assumed to be perfect. The second step is to orientate component 3 to minimise the eccentricity based on variations in component 3 together with the residual variation resulting from the first step. The stage-by-stage nature of this process makes its implementation straightforward and directly relevant to stage-by-stage assembly.

Using the notation developed earlier, the minimum eccentricity is approximated as:

$$\varepsilon_3^{\min} \approx \min_{\theta_{Z3}} \left| r_3^{(3)} \exp\left(i\gamma_3^{(3)}\right) + \min_{\theta_{Z2}} \left| r_2^{(3)} \exp\left(i\gamma_2^{(3)}\right) + r_1^{(3)} \exp\left(i\gamma_1^{(3)}\right) \right| \right|. \tag{33}$$

Using Eqs. (23)–(25) and (27) in Eq. (33), it can be shown that the *approximate* minimum eccentricity can be written as:

$$\varepsilon_3^{\min} = \left| \left| r_1^{(3)} - r_2^{(3)} \right| - r_3^{(3)} \right| = \left| \left| \begin{array}{r} \sqrt{\left(\mathrm{d}X_1 + \mathrm{d}\theta_{Y1}(Z_2+Z_3)\right)^2 + \left(\mathrm{d}Y_1 - \mathrm{d}\theta_{X1}(Z_2+Z_3)\right)^2} \\ -\sqrt{\left(\mathrm{d}X_2 + \mathrm{d}\theta_{Y2}Z_3\right)^2 + \left(\mathrm{d}Y_2 - \mathrm{d}\theta_{X2}Z_3\right)^2} \end{array} \right| - \sqrt{\mathrm{d}X_3^2 + \mathrm{d}Y_3^2} \right|. \tag{34}$$

For an n-component assembly, the approximate approach proposed for three components is generalised. In this case, an $(n-1)$ step "stage-by-stage" approach is used. The first step is to select the orientation of component 2 to minimise the eccentricity based on variations in components 1 and 2 only, with all subsequent components assumed to be perfect. The second step is to orientate component 3 to minimise the eccentricity based on variations in component 3 together with the residual variation resulting from the first step, and all subsequent components assumed to be perfect. Generalising this procedure, the jth step is to orientate component $(j+1)$ to minimise the eccentricity based on variations in component $(j+1)$ together with the residual variation remaining after the $(j-1)$th step, assuming all subsequent components are perfect. Applying this procedure to the whole assembly, the minimum eccentricity can be approximated as:

$$\varepsilon_n^{\min} \approx \min_{\theta_{Zn}} \left| r_n^{(n)} \exp\left(i\gamma_n^{(n)}\right) + \min_{\theta_{Zn-1}} \left| r_{n-1}^{(n)} \exp\left(i\gamma_{n-1}^{(n)}\right) + \ldots + \min_{\theta_{Z2}} \left| r_2^{(n)} \exp\left(i\gamma_2^{(n)}\right) + r_1^{(n)} \exp\left(i\gamma_1^{(n)}\right) \right) \right| \right| \tag{35}$$

Following the above procedure and using Eq. (35), it can be shown that the approximate minimum eccentricity can be expressed as:

$$\varepsilon_n^{\min} = \left| \ldots \left| \left| r_1^{(n)} - r_2^{(n)} \right| - r_3^{(n)} \right| - r_4^{(n)} \right| - \ldots - r_n^{(n)} \Big|. \tag{36}$$

Unlike WBA, the proposed BBA (for $n>3$) is an approximate method based on the components being assembled stage by stage. This approach is well suited to practical assembly procedures and always produces eccentricities that are greater than or equal to the actual minimum value. The expressions (28)–(36) derived in this section are used next to develop analytical expressions for the pdf of the eccentricity for the nth component in an assembly.

3 A probabilistic approach for straight-build assembly

When analysing the assembly of axi-symmetric components, it is useful to quantify the likelihood that the eccentricity exceeds a particular level. In this section, the dimensional variations $\mathrm{d}X_i$, $\mathrm{d}Y_i$, $\mathrm{d}\theta_{Xi}$, $\mathrm{d}\theta_{Yi}$ for each component are modelled as random variables and pdfs are developed for the eccentricities developed using DBA, BBA and WBA. The pdfs obtained for the different build scenarios provide a useful insight into the improvements gained using the different approaches. The pdfs are then used to calculate the probability that the build eccentricity exceeds a particular threshold value.

The component variations (translation $\mathrm{d}X_i$, $\mathrm{d}Y_i$ and rotation $\mathrm{d}\theta_{Xi}$, $\mathrm{d}\theta_{Yi}$) used to predict the eccentricity are assumed to be statistically independent, zero-mean

Gaussian random variables with known standard deviations such that: $E\left[\mathrm{d}X_i^2\right]=\sigma_{Xi}^2$, $E\left[\mathrm{d}Y_i^2\right]=\sigma_{Yi}^2$, $E\left[\mathrm{d}\theta_{Xi}^2\right]=\sigma_{\theta Xi}^2$ and $E\left[\mathrm{d}\theta_{Yi}^2\right]=\sigma_{\theta Yi}^2$, where σ_{Xi}, σ_{Yi}, $\sigma_{\theta Xi}$ and $\sigma_{\theta Yi}$ are standard deviations for variations in the location and orientation of the mating features for the *i*th component. In what follows, it is assumed that: $\sigma_{Yi}=\sigma_{Xi}$ and $\sigma_{\theta Xi}=\sigma_{\theta Yi}=\sigma_{\theta i}$.

3.1 Direct build assembly

As the Gaussian random component variations are statistically independent, it can be shown that the terms $\left(\sum_{i=1}^{n}\mathrm{d}X_i+\sum_{i=1}^{n-1}\mathrm{d}\theta_{Yi}\sum_{j=i+1}^{n}Z_j\right)$ and $\left(\sum_{i=1}^{n}\mathrm{d}Y_i-\sum_{i=1}^{n-1}\mathrm{d}\theta_{Xi}\sum_{j=i+1}^{n}Z_j\right)$ appearing in Eq. (28) are statistically independent and Gaussian distributed. It can also be shown that the standard deviations for both these terms are: $\sqrt{\sum_{i=1}^{n}\sigma_{Xi}^2+\sum_{i=1}^{n=1}\sigma_{\theta i}^2\left(\sum_{j=i+1}^{n}Z_j\right)^2}$.

Using Eq. (28) and a change of variables, it can be shown that the pdf of the eccentricity ε_n^{Direct}, for the final component in an assembly consisting of *n* axi-symmetric components, is given by:

$$p\left(\varepsilon_n^{\mathrm{Direct}}\right)=\begin{cases}\frac{\varepsilon_n^{\mathrm{Direct}}}{\sigma_n^2}\exp\left(-\frac{\left(\varepsilon_n^{\mathrm{Direct}}\right)^2}{2\sigma_n^2}\right), & \varepsilon_n^{\mathrm{Direct}}\geq 0\\ 0 & \text{otherwise}\end{cases}\tag{37}$$

where

$$\sigma_n=\sqrt{\sum_{i=1}^{n}\sigma_{Xi}^2+\sum_{i=1}^{n-1}\sigma_{\theta i}^2\left(\sum_{j=i+1}^{n}Z_j\right)^2}\tag{38}$$

and Eq. (37) is a Rayleigh distribution [25].

3.2 Worst build assembly

For a two-component assembly, the maximum build eccentricity $\varepsilon_2^{\max}$ is given by Eq. (29). Noting that $\mathrm{d}X_1+\mathrm{d}\theta_{Y1}Z2$ and $\mathrm{d}Y_1-\mathrm{d}\theta_{X1}Z2$ are zero-mean Gaussian-independent random variables, it follows that $\sqrt{\left(\mathrm{d}X_1+\mathrm{d}\theta_{Y1}\,Z_2\right)^2+\left(\mathrm{d}Y_1-\mathrm{d}\theta_{X1}\,Z_2\right)^2}$ has a Rayleigh distribution. Given that $\sqrt{\mathrm{d}X_2^2+\mathrm{d}Y_2^2}$ and $\sqrt{\left(\mathrm{d}X_1+\mathrm{d}\theta_{Y1}\,Z_2\right)^2+\left(\mathrm{d}Y_1-\mathrm{d}\theta_{X1}\,Z_2\right)^2}$ are statistically independent and the distributions are each known (both Rayleigh), the pdf for the maximum eccentricity $\varepsilon_2^{\max}$ can be obtained using a change of variables [25]. Using this approach, it can be shown that the pdf for $\varepsilon_2^{\max}$ is given by:

$$p\left(\varepsilon_2^{\max}\right)=\begin{cases}\frac{1}{\sigma_2^4}\exp\left(-\frac{\left(\varepsilon_2^{\max}\right)^2}{2\sigma_2^2}\right)\{\sqrt{2\pi}\left[\left(\varepsilon_2^{\max}\right)^2-\sigma_2^2\right]\frac{\sigma_{2,1}^*\,\sigma_{X2}}{\sigma_2}[\Phi\left(\frac{\varepsilon_2^{\max}\,\sigma_{2,1}^*}{\sigma_{X2}\,\sigma_2}\right)+ & \\ \Phi\left(\frac{\varepsilon_2^{\max}\sigma_{x2})}{\sigma_{2,1}^*\,\sigma_2}\right)-1]+\varepsilon_2^{\max}\,{\sigma_{2,1}^*}^2\,e^{-\frac{\left(\varepsilon_2^{\max}\right)^2\sigma_{X2}^2}{2{\sigma_{2,1}^*}^2\sigma_2^2}}+\varepsilon_2^{\max}\,\sigma_{X2}^2\,e^{-\frac{\left(\varepsilon_2^{\max}\right)^2{\sigma_{2,1}^*}^2}{2\sigma_{X2}^2\sigma_2^2}}\}, & \varepsilon_2^{\max}\geq 0\\ 0 & \text{otherwise}\end{cases}\tag{39}$$

where σ_2 is obtained using Eq. (38) with $n=2$, $\sigma_{2,1}^*=\sqrt{\sigma_{X1}^2+\sigma_{\theta 1}^2Z_2^2}$ and Φ is the cumulative normal distribution (which can be obtained from the error function [25]).

For a three-component assembly, the maximum build eccentricity $\varepsilon_3^{\max}$ is given by Eq. (30). Noting that $\mathrm{d}X_1+\mathrm{d}\theta_{Y1}(Z_2+Z_3)$, $\mathrm{d}Y_1-\mathrm{d}\theta_{X1}(Z_2+Z_3)$, $\mathrm{d}X_2+\mathrm{d}\theta_{Y2}Z_3$ and $\mathrm{d}Y_2-\mathrm{d}\theta_{X2}Z_3$ are zero-mean Gaussian-independent random variables, it follows that $\sqrt{\left[\mathrm{d}X_1+\mathrm{d}\theta_{Y1}(Z_2+Z_3)\right]^2+\left[\mathrm{d}Y_1-\mathrm{d}\theta_{X1}(Z_2+Z_3)\right]^2}$, $\sqrt{\left(\mathrm{d}X_2+\mathrm{d}\theta_{Y2}Z_3\right)+\left(\mathrm{d}Y_2-\mathrm{d}\theta_{X2}Z_3\right)}$ and $\sqrt{\mathrm{d}X_3^2+\mathrm{d}Y_3^2}$ are all Rayleigh distributions. Given that the distributions are known, the pdf for the maximum eccentricity $\varepsilon_3^{\max}$ can also be obtained using a change of variables [25]. Using this approach, it can be shown that the pdf for $\varepsilon_{\max}^3$ is given by:

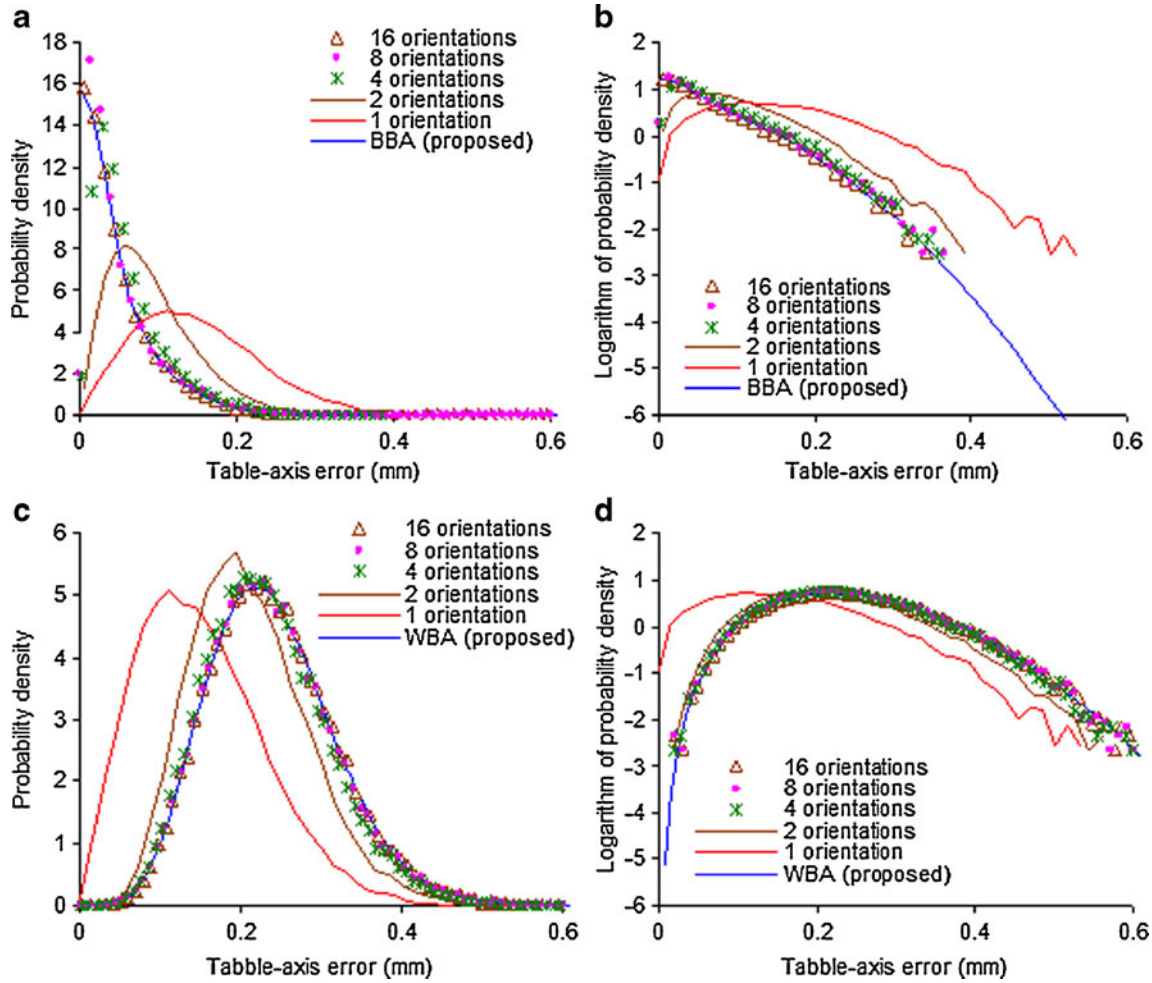

Fig. 5 Comparisons of probability density function of eccentricity for the proposed approach and Monte Carlo simulations with the different orientations for three-component-build eccentricity with tolerance 0.1 mm: **a** best build assembly with linear scale, **b** best build assembly with semi-log scale, **c** worst build assembly with linear scale and **d** worst build assembly with semi-log scale

$$p\left(\varepsilon_3^{\max}\right)=\begin{cases}\displaystyle\int_0^{\varepsilon_3^{\max}}\frac{\left(\varepsilon_3^{\max}-x\right)\exp\left(-\frac{x^2}{2\sigma_3^2}-\frac{\left(\varepsilon_3^{\max}-x\right)^2}{2\sigma_{X3}^2}\right)}{\sigma_3^2 2\sigma_{X3}^2}\left\{\sqrt{2\pi}\left(x^2-\sigma_3^2\right)\frac{\sigma_{3,1}^*\sigma_{3,2}^*}{\sigma_3}\left[\Phi\left(\frac{x\sigma_{3,1}^*}{\sigma_{3,2}^*\,\sigma_3}\right)\right.\right. & \varepsilon_3^{\max}\geq 0\\ \left.\left.+\Phi\left(\frac{x\sigma_{3,2}^*}{\sigma_{3,1}^*\sigma_3}\right)-1\right]+x\,{\sigma_{3,1}^*}^2\exp\left(-\frac{x^2\,{\sigma_{3,2}^*}^2}{2\,{\sigma_{3,1}^*}^2\,\sigma_3^2}\right)+x\,{\sigma_{3,2}^*}^2\exp\left(-\frac{x^2\,{\sigma_{3,1}^*}^2}{2\,{\sigma_{3,2}^*}^2\,\sigma_3^2}\right)\right\}dx, & \\ 0 & \text{otherwise}\end{cases} \tag{40}$$

where $\sigma_{3,1}^*=\sqrt{\sigma_{X1}^2+\sigma_{\theta1}^2\left(Z_2+Z_3\right)^2}$ and $\sigma_{3,2}^*=\sqrt{\sigma_{X2}^2+\sigma_{\theta2}^2 Z_3^2}$. In a similar way, the pdf for the worst build assembly for an n-component assembly can be developed.

3.3 Best build assembly

For a two-component assembly, the minimum eccentricity is given by Eq. (32). Using a similar approach to that

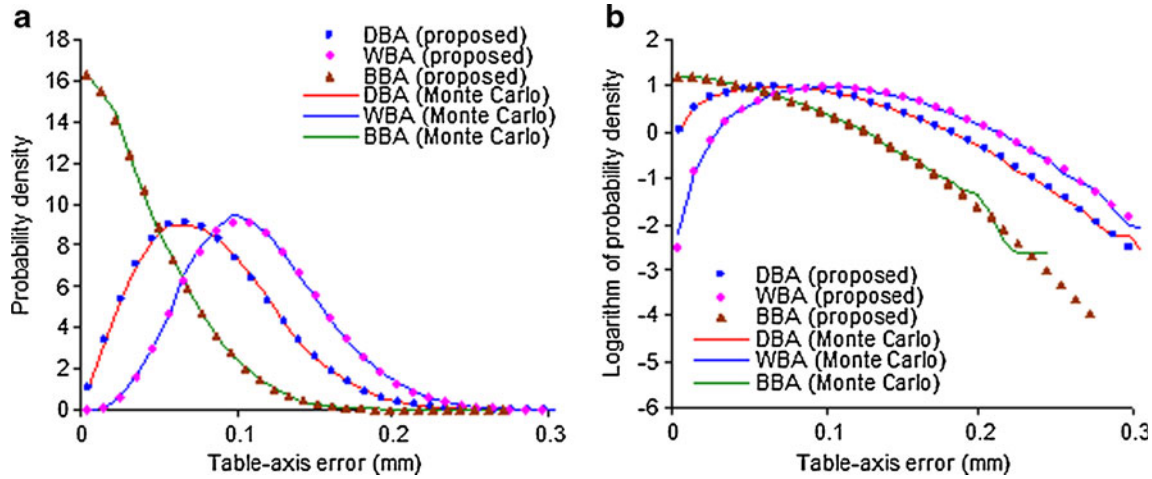

Fig. 6 Probability density function for two-component build eccentricity with tolerance 0.1 mm: **a** linear scale and **b** semi-log scale

presented earlier for a two-component assembly using WBA, it can be shown that the pdf for $\varepsilon_2^{\min}$ is given by:

$$p\left(\varepsilon_2^{\min}\right) = \begin{cases} \frac{1}{\sigma_2^4}\exp\left(-\frac{\left(\varepsilon_2^{\min}\right)^2}{2\sigma_2^2}\right)\left\{\sqrt{2\pi}\left[\left(\varepsilon_2^{\min}\right)^2-\sigma_2^2\right]\frac{\sigma_{2,1}^*\,\sigma_{X2}}{\sigma_2}\left[\Phi\left(\frac{\varepsilon_2^{\min}\,\sigma_{2,1}^*}{\sigma_{X2}\,\sigma_2}\right)+\right.\right. \\ \left.\left.\Phi\left(\frac{\varepsilon_2^{\min}\,\sigma_{X2}}{\sigma_{2,1}^*\,\sigma_2}\right)-2\right]+\varepsilon_2^{\min}\,{\sigma_{2,1}^*}^2\,e^{-\frac{\left(\varepsilon_2^{\min}\right)^2\sigma_{X2}^2}{2{\sigma_{2,1}^*}^2\sigma_2^2}}+\varepsilon_2^{\min}\,\sigma_{X2}^2\,e^{-\frac{\left(\varepsilon_2^{\min}\right)^2{\sigma_{2,1}^*}^2}{2\sigma_{X2}^2\sigma_2^2}}\right\}, & \varepsilon_2^{\min}\geq 0 \\ 0 & \text{otherwise} \end{cases} \tag{41}$$

where the notation used is the same as in Eq. (39).

For a three-component assembly, the *approximate* minimum eccentricity is given by Eq. (34). Using a similar approach to that presented earlier for WBA, it can be shown that the pdf for $\varepsilon_3^{\min}$ is given by:

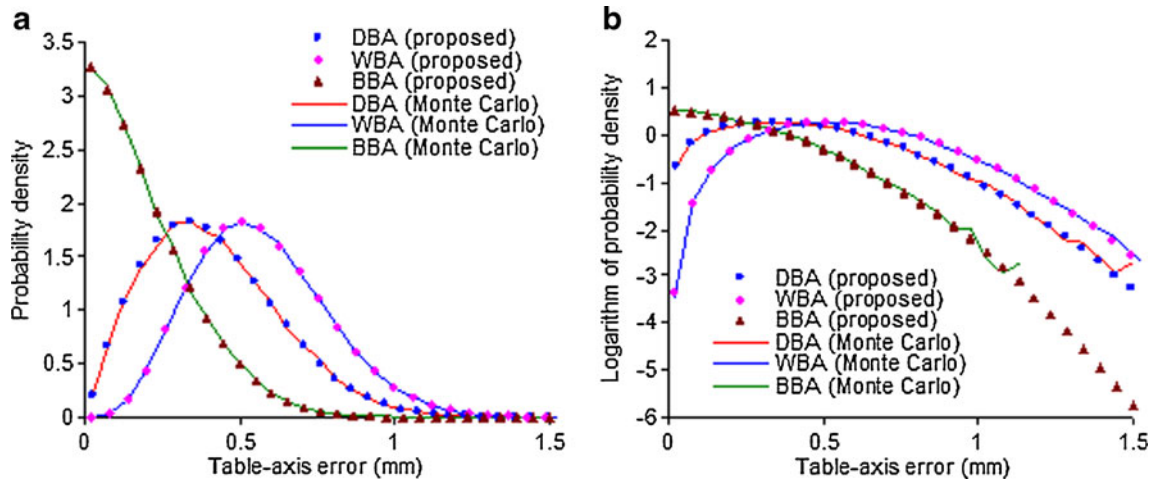

Fig. 7 Probability density function for two-component build eccentricity with tolerance 0.5 mm: **a** linear scale and **b** semi-log scale

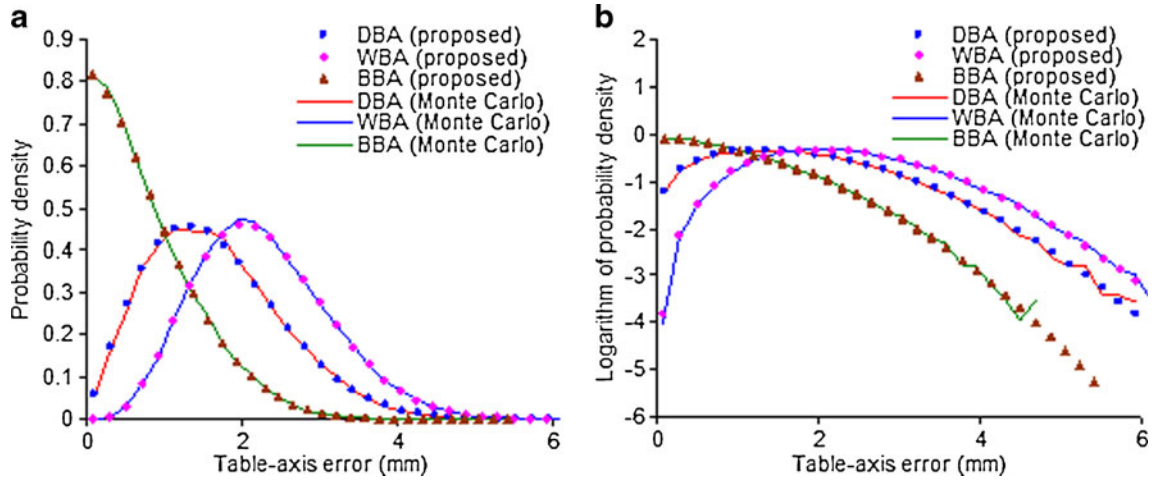

Fig. 8 Probability density function for two-component build eccentricity with tolerance 2.0 mm: **a** linear scale and **b** semi-log scale

$$
p\left(\varepsilon_3^{\min}\right)=\begin{cases}
\displaystyle\int_0^{\infty}\frac{x+\varepsilon_3^{\min}}{\sigma_{X3}^2}\,e^{-\frac{\left(x+\varepsilon_3^{\min}\right)^2}{2\sigma_{X3}^2}}\frac{e^{-\frac{x^2}{2\sigma_3^2}}}{\sigma_3^4}\left\{\sqrt{2\pi}\left(x^2-\sigma_3^2\right)\frac{\sigma_{3,1}^*\sigma_{3,2}^*}{\sigma_3}\left[\Phi\left(\frac{x\sigma_{3,1}^*}{\sigma_{3,2}^*\sigma_3}\right)\right.\right.\\
\qquad\left.\left.+\Phi\left(\frac{x\sigma_{3,2}^*}{\sigma_{3,1}^*\sigma_3}\right)-2\right]+x\,{\sigma_{3,2}^*}^2\,e^{-\frac{x^2{\sigma_{3,1}^*}^2}{2{\sigma_{3,2}^*}^2\sigma_3^2}}+x\,{\sigma_{3,1}^*}^2\,e^{-\frac{x^2{\sigma_{3,2}^*}^2}{2{\sigma_{3,1}^*}^2\sigma_3^2}}\right\}\mathrm{d}x\\
+\displaystyle\int_{\varepsilon_3^{\min}}^{\infty}\frac{x-\varepsilon_3^{\min}}{\sigma_{X3}^2}\,e^{-\frac{\left(x-\varepsilon_3^{\min}\right)^2}{2\sigma_{X3}^2}}\frac{e^{-\frac{x^2}{2\sigma_3^2}}}{\sigma_3^4}\left\{\sqrt{2\pi}\left(x^2-\sigma_3^2\right)\frac{\sigma_{3,1}^*\sigma_{3,2}^*}{\sigma_3}\left[\Phi\left(\frac{x\sigma_{3,1}^*}{\sigma_{3,2}^*\sigma_3}\right)\right.\right. & \varepsilon_3^{\min}\geq 0\\
\qquad\left.\left.+\Phi\left(\frac{x\sigma_{3,2}^*}{\sigma_{3,1}^*\sigma_3}\right)-2\right]+x\,{\sigma_{3,2}^*}^2\,e^{-\frac{x^2{\sigma_{3,1}^*}^2}{2{\sigma_{3,2}^*}^2\sigma_3^2}}+x\,{\sigma_{3,1}^*}^2\,e^{-\frac{x^2{\sigma_{3,2}^*}^2}{2{\sigma_{3,1}^*}^2\sigma_3^2}}\right\}\mathrm{d}x,\\
0 & \text{otherwise}
\end{cases}
\tag{42}
$$

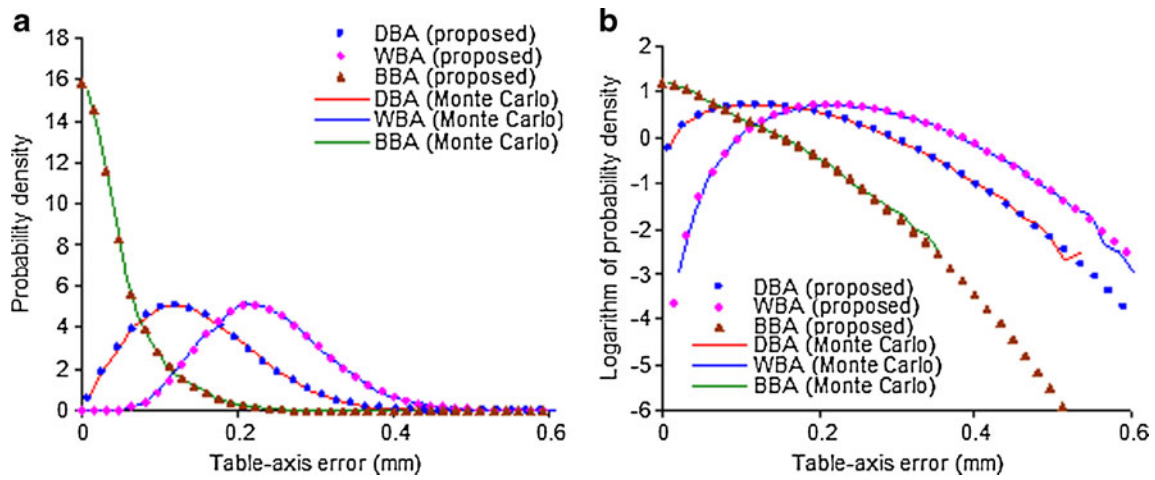

Fig. 9 Probability density function for three-component build eccentricity with tolerance 0.1 mm: **a** linear scale and **b** semi-log scale

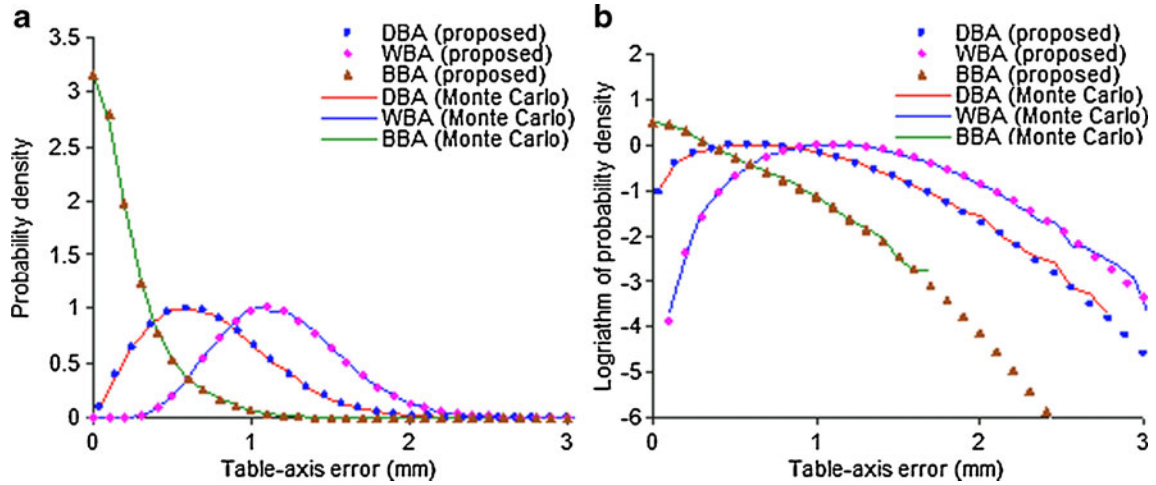

Fig. 10 Probability density function for three-component build eccentricity with tolerance 0.5 mm: **a** linear scale and **b** semi-log scale

where the notation used is the same as in Eq. (40). In a similar way, the pdf for the best build assembly for an *n*-component assembly can be developed.

4 Numerical examples

The initial two examples investigated consider: (a) a two-component assembly and (b) a three-component assembly. In both of these examples, all components are axi-symmetric (cylindrical) with nominal height H=70 mm and nominal diameter W=100 mm. These dimensions ensure that for each component, the nominal mating feature on the upper surface have coordinates [0,0,70] relative to the mating feature on the lower surface, i.e. X_i=0 mm, Y_i= 0 mm, Z_i=70 mm. Dimensional tolerances are specified for the location (dX_i, dY_i and dZ_i) and orientation $d\theta_{Xi}$, $d\theta_{Yi}$ and $d\theta_{Zi}$ of the mating feature for each component on its upper surface relative to its lower surface, and the variations are assumed to be zero-mean Gaussian random variables, where the standard deviation (σ) is taken to be one third of the specified tolerance. The influence of different component tolerances on the eccentricity of the build is assessed, and the tolerance values chosen for the component heights h_i (=dX_i=dY_i=dZ_i) are 0.1, 0.5 and 2 mm. The tolerances for component diameters are assumed to take the same values as those for the component heights. The tolerances for the orientation error of the upper surface relative to the lower surface for each component are taken to be: $\frac{2h_i}{W}$, $\frac{2h_i}{W}$ and $\frac{2dX_i}{W}$ about the *X*-, *Y*- and *Z*-axes, respectively [22].

Numerical results obtained using the proposed probabilistic methods are compared with results obtained using the

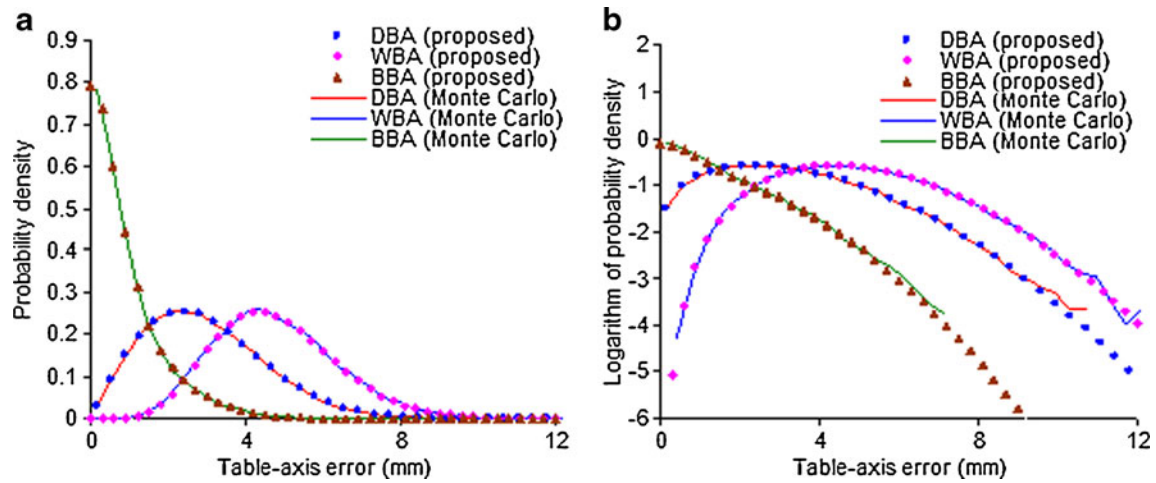

Fig. 11 Probability density function for three-component-build eccentricity with tolerance 2.0 mm: **a** linear scale and **b** semi-log scale

Table 1 Comparison of the execution time for the proposed method and Monte Carlo simulations for two-component and three-component assemblies

Number of components	Assembly procedures	Execution time
2	Direct build assembly (proposed)	1.0
	Worst build assembly (proposed)	1.2
	Best build assembly (proposed)	1.2
	Direct build assembly (Monte Carlo)	140.8
	Worst build assembly (Monte Carlo)	185.4
	Best build assembly (Monte Carlo)	185.4
3	Direct build assembly (proposed)	1.0
	Worst build assembly (proposed)	25.2
	Best build assembly (proposed)	50.6
	Direct build assembly (Monte Carlo)	180.2
	Worst build assembly (Monte Carlo)	285.8
	Best build assembly (Monte Carlo)	285.8

standard Monte Carlo simulation method. Convergence studies have been performed to determine the number of simulations required by a Monte Carlo simulation to obtain accurate results. For the examples considered, it was found that 100,000 simulations were required to obtain predictions for the mean, standard deviation, skewness and kurtosis to be accurate to within ±1 %. An advantage of the proposed probabilistic approach over Monte Carlo simulation is that it does not require a convergence study to be performed.

As described in Section 2, the analysis developed for BBA and WBA is based on using linearised equations and a stage-by-stage "optimisation" in which the orientation of a component about its central axis is chosen to minimise or maximise the eccentricity, respectively. In practical assemblies, each component only has a finite number of possible orientations (indexing positions) from which to choose. To validate the linearisation approach used and investigate the influence of using a limited number of orientations, the proposed approach has been compared with Monte Carlo simulations based on Eq. (17) and using only 2, 4, 8 and 16 uniform orientations. The results obtained for the three-component assembly with a tolerance of 0.1 mm are plotted on both linear and log-axes, as shown in Fig. 5a, b for BBA and in Fig. 5c, d for WBA. These results compare the pdfs on linear and logarithmic axes for the eccentricity of the final component in the complete assembly. The results obtained using a single orientation are obtained using the DBA result (Eq. (37)), whilst those obtained using two orientations were obtained using the approach developed in Yang et al. (submitted for publication) for two-dimensional assemblies. As expected, improved agreement is obtained between Monte Carlo simulation and the proposed approaches as the number of available orientations increases. In particular, with eight orientations, the agreement is good, whilst with 16 orientations, the agreement is excellent. These results suggest that the proposed approach is valid for eight or more indexing positions, whilst the fact that these results are in such good agreement with the proposed approach also validates the linearisation approach used.

In what follows, Monte Carlo simulation results are obtained using Eqs. (28), (31) and (36) and are based on linearised equations and unlimited orientations, for DBA, WBA and BBA, respectively. To confirm the accuracy of the proposed approach, the pdfs are plotted on both linear and logarithmic axes. Figures 6, 7, 8, 9, 10 and 11 compare

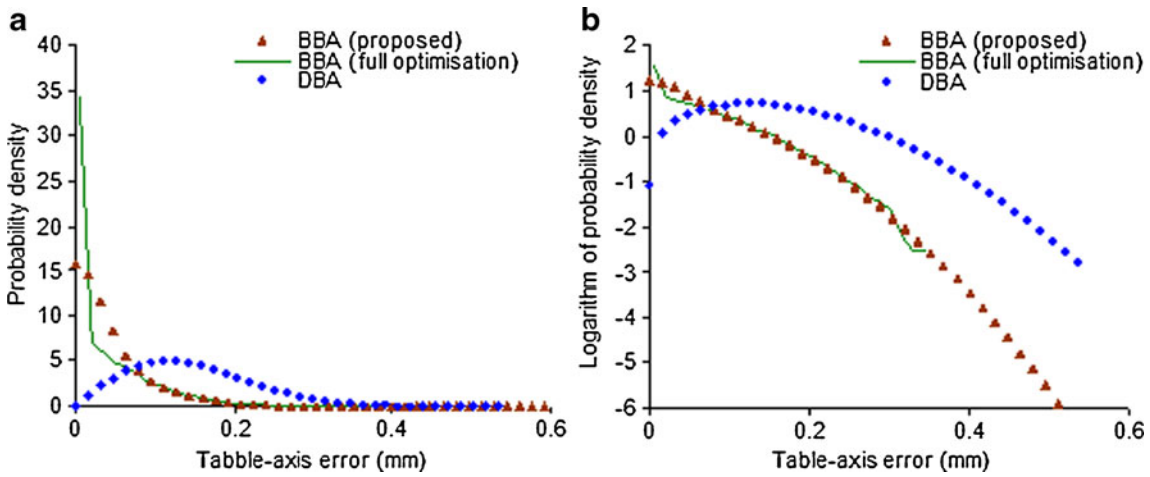

Fig. 12 Probability density function for eccentricity of a three-component assembly with tolerance 0.1 mm: **a** linear scale and **b** semi-log scale

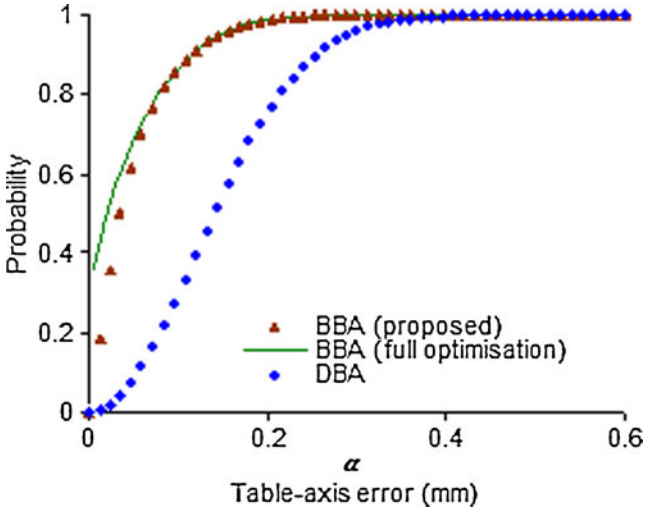

Fig. 13 Probability that the build eccentricity does not exceed a value α for three-component assembly with tolerance 0.1 mm

the proposed approach with Monte Carlo simulation for the two-component assembly (Figs. 6, 7 and 8) and the three-component assembly (Figs. 9, 10 and 11) with different component tolerance values. From Figs. 6, 7, 8, 9, 10 and 11, it is clear that all statistical distributions are highly non-Gaussian, and the results obtained using the proposed approach are in excellent agreement with Monte Carlo simulations. It should be noted that the agreement at the tails of the log-pdf is not as good because the Monte Carlo simulations are less accurate for high eccentricities. This deficiency of the Monte Carlo method serves to highlight one of the advantages offered by the derived pdf expressions, which are valid for all eccentricity values. The results

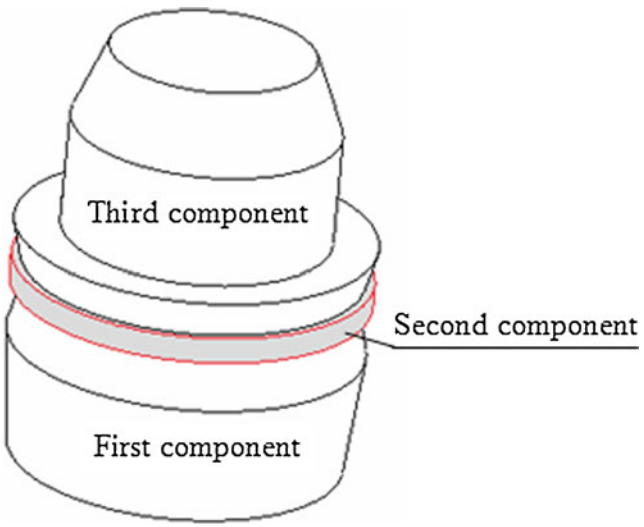

Fig. 14 Schematic drawing of three non-identical components assembly

confirm that the derived analytical pdf expressions (Eqs. (37) and (39)–(42)) are valid.

The results also indicate that as the tolerance increases from a small value (0.1 mm) to a large value (2.0 mm), the magnitude of the eccentricity increases and the general shape of the distributions remains relatively unchanged. This is not surprising for direct build assembly, as the distribution is always Rayleigh.

The efficiency of the proposed methods is assessed by comparing the execution times required to perform the calculations with results obtained using Monte Carlo simulations. Table 1 shows CPU times (normalized relative to DBA) for the results shown in Figs. 6 and 9—similar trends were observed for the other cases considered.

It is clear from Table 1 that the proposed probabilistic approach is much more efficient than Monte Carlo simulations, and the DBA calculation is the most efficient of all. This is because the pdf can be calculated easily using Eq. (37) for any number of components. The proposed WBA and BBA results are achieved much more efficiently for a two-component assembly than for a three-component assembly. For example, the calculation load for the proposed WBA and BBA for the three-component assembly is increased by factors of 21 and 42, respectively, compared to the two-component assembly. The reason for this is that Eqs. (40) and (42) involve additional integrations compared to Eqs. (39) and (41), respectively. As the number of components increases, the number of embedded integrals increases, making the proposed method less efficient. However, the results in Table 1 indicate that for two- and three-component assemblies, the proposed method is much more efficient than Monte Carlo simulations. The Monte Carlo simulation results are based on performing 100,000 simulations, and the CPU times associated with these results can be reduced by simply reducing the number of simulations. However, reducing the number of simulations will adversely affect the accuracy of the results.

5 Discussion and application to a realistic assembly

5.1 Comparison of the proposed best build assembly and Monte Carlo simulation using a full-optimisation approach

As described in Section 2, BBA is based on re-orientating individual components on a stage-by-stage basis, rather than using a full optimisation. Figure 12 compares results obtained using the proposed stage-by-stage BBA with full optimisation and DBA for a three-component assembly with a tolerance of 0.1 mm. It is clear that BBA and a full optimisation yield improved quality assemblies compared

Table 2 Dimensions of each component

Component	Height (mm)	Base diameter (mm)	Top diameter (mm)
First component	200	400	500
Second component	10	500	500
Third component	400	500	300

to DBA. It can also be seen that the results obtained using BBA and full optimisation are in reasonable agreement but differ for small eccentricities, with the full optimisation method yielding a higher proportion of smaller eccentricity assemblies than the stage-by-stage BBA approach. This is expected as the full optimisation is guaranteed to produce assemblies with eccentricities that are less than or equal to those produced by BBA. However, the agreement at larger eccentricities is good.

One of the main reasons for calculating the pdf for the eccentricity is to predict the probability that the eccentricity is less than a particular value. The probability $P(\alpha)$ that the eccentricity ε does not exceed a value α is given by:

$$P(\alpha) = \int_0^{\alpha} p(\varepsilon)\mathrm{d}\varepsilon, \tag{43}$$

where $p(\varepsilon)$ is the probability density function for the eccentricity. Figure 13 plots the probability obtained using Eq. (43) for the example considered in Fig. 12.

These results confirm that BBA and full optimisation always yield a much higher proportion of assemblies with reduced eccentricity compared to DBA. It can also be seen that the results obtained using the proposed BBA approach agree well with the full optimisation results, particularly as the eccentricity increases.

5.2 Application to a realistic assembly

In this section, the proposed methods are applied to a sub-assembly, originating in aero-engines to illustrate a more

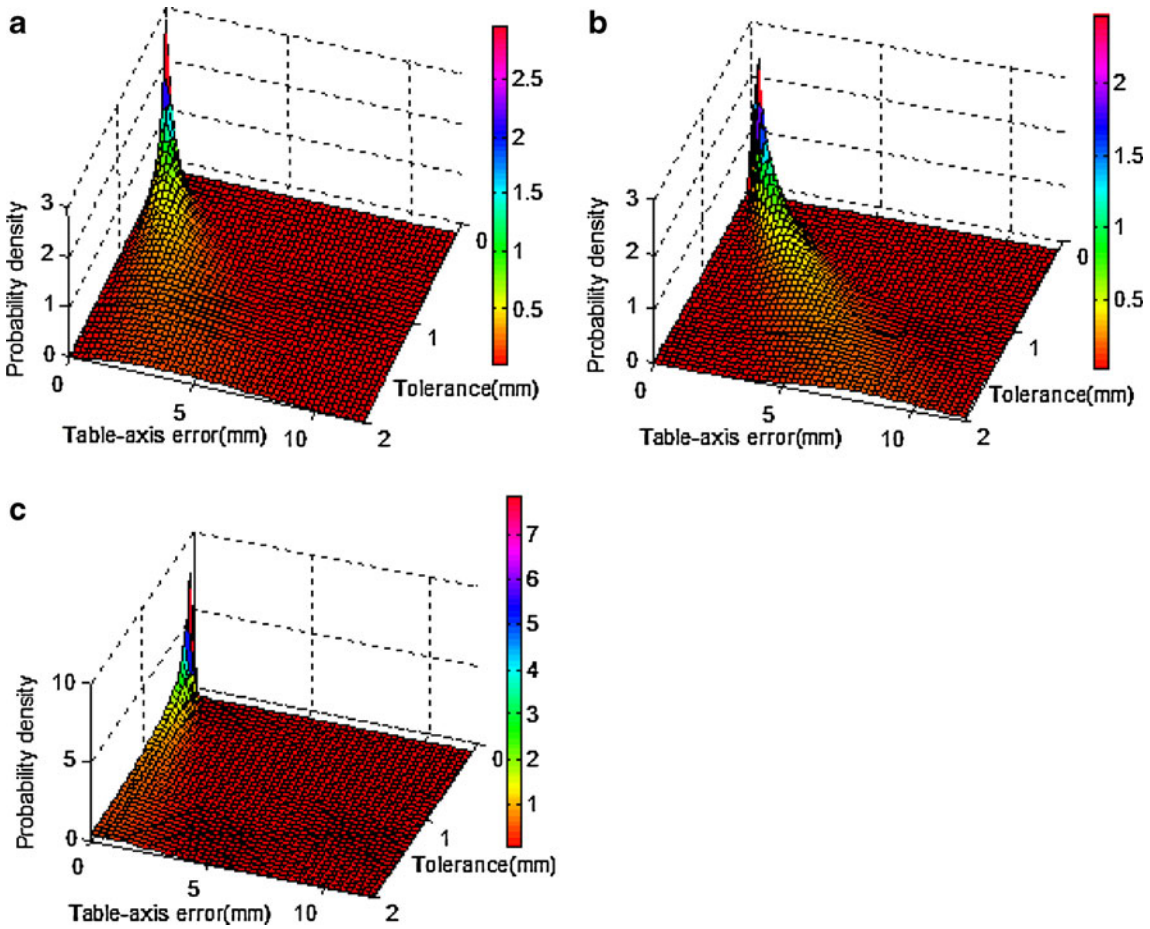

Fig. 15 Probability density against given table-axis error and tolerance for the different assembly procedures: **a** direct build assembly, **b** worst build assembly and **c** best build assembly

realistic assembly. The example of an aero-engine assembly consists of three non-identical axi-symmetric components, as shown in Fig. 14. The adopted dimensions of each component are listed in Table 2. Each component is designed so that it can be orientated in 16 different positions, and the diameter and height of each component is defined in terms of tolerances. The manufacturing variations are assumed to be zero-mean Gaussian random variables with standard deviation (σ) equal to one third of the tolerance value, and in this example, the tolerances for the diameter and height are selected to have the same value. DBA, WBA and BBA have been used to determine the pdfs for the eccentricity using different tolerance values, and the results are shown in Fig. 15. The results indicate that the table-axis error (eccentricity) greatly depends on the assembly procedure and the assigned tolerance value. As expected, smaller tolerance values ensure there is less variation in the table-axis error, and BBA provides the best performance of the three assembly procedures considered.

The calculated pdfs are used in conjunction with Eq. (42) to calculate the table-axis errors corresponding to probabilities of 95 and 99.5 % for different component tolerances. Figure 16 shows plots of the table-axis error versus component tolerance for the 95 and 99.5 % confidence regions. In both cases, it can be seen that there is a linear relationship between table-axis error and the component tolerance. These results indicate that for the table-axis error to be less than 1 mm with 95 % confidence, the component tolerances must be less than 0.32 mm for WBA, less than 0.42 mm for DBA and less than 1.15 mm for BBA, respectively, whilst to achieve the same table-axis error with 99.5 % confidence requires the component tolerance to be less than 0.26 mm for WBA, less than 0.32 mm for DBA and less than 0.72 mm for BBA, respectively. These results clearly indicate that BBA can be used to achieve the same quality as DBA and WBA but using much larger component tolerances.

6 Summary and conclusions

Models describing the straight-build assembly of rigid axi-symmetric components have been presented. These models are based on connective assembly models and use a linearisation procedure to develop analytical expressions for the eccentricity of the assembly. The developed expressions were used to analyse three different build scenarios: (a) DBA, (b) BBA and (c) WBA for assemblies composed of three-dimensional axi-symmetric components. BBA and WBA are based on rotating each component and selecting the orientations that minimise and maximise (respectively) the eccentricity of the final assembly. In contrast, DBA does not attempt to optimise the assembly process at all. Exact expressions for the eccentricity were developed for DBA and WBA. However, it was not possible to develop exact expressions for BBA when the assembly had three or more components, and in this case, approximate expressions were developed. The eccentricity expressions were used together with the assumption that the component variations are independent Gaussian random variables to derive probability density functions for the eccentricity (table-axis error) of the complete assembly using the different build scenarios. DBA produces eccentricities having a Rayleigh distribution, whilst BBA and WBA produce eccentricities with a non-standard form. In principle, the BBA and WBA pdfs can be developed for an assembly having any number of components, but only results for two- and three-component assemblies were considered. Numerical examples

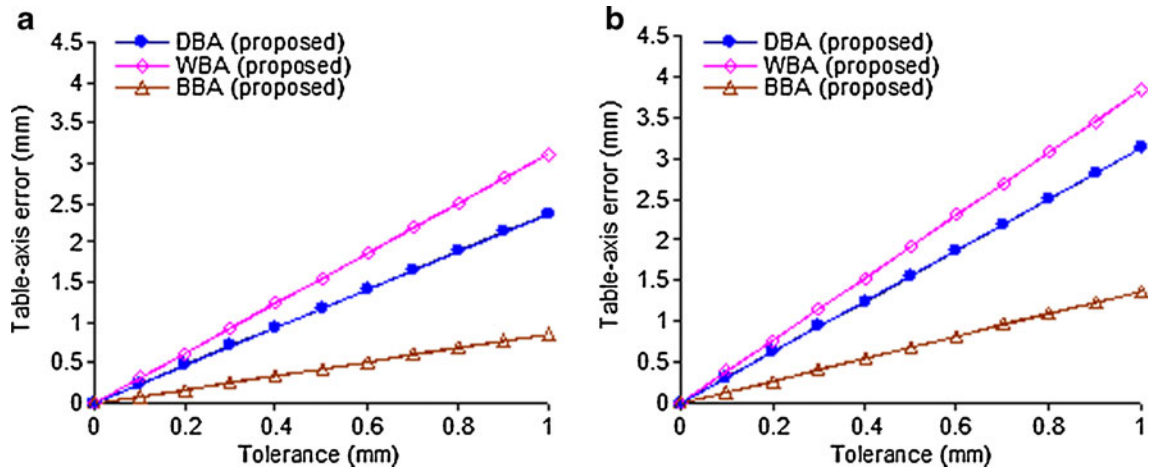

Fig. 16 Three-component build eccentricity is within at 95 and 99.5 % confidence regions for the different tolerances: **a** 95 % confidence region and **b** 99.5 % confidence region

were used to validate the accuracy and demonstrate the improved efficiency of the proposed approaches compared to Monte Carlo simulations, for two- and three-component assemblies. The final example applies the proposed techniques to a more realistic case originating in aero-engine subassembly, and the results serve to highlight the benefits of using BBA to improve build quality compared to DBA and to demonstrate that the probabilistic approach provides a valuable tool in industrial applications.

Acknowledgments The authors gratefully acknowledge financial support from the Engineering and Physical Sciences Research Council through Nottingham Innovative Manufacturing Research Centre. The authors also gratefully acknowledge the help and advice provided by Mat Yates and Steve Slack at Rolls-Royce plc at the early stage of this work.

References

1. Mantripragada R, Whitney DE (1999) Modeling and controlling variation propagation in mechanical assemblies using state transition models. IEEE Trans Robot Autom 15:124–140
2. Lin CY, Huang WH, Jeng MC, Doong JL (1997) Study of an assembly tolerance allocation model based on Monte Carlo simulation. J Mater Process Technol 70:9–16
3. Thimm G, Britton G, Cheong FS (2001) Controlling tolerance stacks for efficient manufacturing. Int J Adv Manuf Technol 18:44–48
4. Forouraghi B (2002) Worst-case tolerance design and quality assurance via genetic algorithms. J Optim Theor Appl 13:251–268
5. Dantan JY, Qureshi AJ (2009) Worst-case and statistical tolerance analysis based on quantified constraint satisfaction problems and Monte Carlo simulation. Comput Aided Des 41:1–12
6. Spolts MF (1971) Design of machine elements. Prentice-Hall, Englewood Cliffs
7. Arron DD, Walter JM, Charles EW (1975) Machine design theory and practices. Macmillan, New York
8. He JR (1991) Estimating the distributions of manufactured dimensions with the beta probability density function. Int J Mach Tool Manuf 31:383–396
9. Nigam SD, Turner JU (1995) Review of statistical approaches to tolerance analysis. Comput Aided Des 27:6–15
10. Wu F, Dantan JY, Etienne A, Siadat A, Martin P (2009) Improved algorithm for tolerance allocation based on Monte Carlo simulation and discrete optimization. Comput Ind Eng 56:1402–1413
11. Toft N, Innocent GT, Gettinby G, Reid SW (2007) Assessing the convergence of Markov Chain Monte Carlo methods: an example from evaluation of diagnostic tests in absence of a gold standard. Prev Vet Med 79:244–256
12. Brooks SP, Gelman A (1998) Alternative methods for monitoring convergence of iterative simulations. J Comput Graph Stat 7:434–455
13. Mustafa YA (2007) A convergence criterion for the Monte Carlo estimates. Simulat Model Pract Theor 15:237–246
14. Jungemann C, Yamaguchi S, Goto H (1997) Convergence estimation for stationary ensemble Monte Carlo simulations. In: International conference on simulation of semiconductor processes and devices, 8–10 Sep 1997, Cambridge, MA, USA
15. Roy U, Li B (1998) Representation and interpretation of geometric tolerances for polyhedral objects-I. Form tolerances. Comput Aided Des 30:151–161
16. Roy U, Li B (1999) Representation and interpretation of geometric tolerances for polyhedral objects-II. Size, orientation and position tolerances. Comput Aided Des 31:273–285
17. Cai M, Yang JX, Wu ZT (2004) Mathematical model of cylindrical form tolerance. Journal of Zhejing University Science 5:890–895
18. Roy U, Liu CR, Woo TC (1991) Review of dimensioning and tolerancing, representation and processing. Comput Aided Des 23:466–483
19. Chen KZ, Feng XA, Lu QS (2002) Intelligent location-dimensioning of cylindrical surfaces in mechanical parts. Comput Aided Des 34:185–194
20. Whitney DE, Gilbert OL (1993) Representation of geometric variations using matrix transforms for statistical tolerance analysis in assemblies. In: Proceedings of the IEEE international conference on robotics and automation, Atlanta, GA, USA
21. Gunston B (1989) Rolls-Royce aero engines. Patrick Stephens, England
22. Whitney DE (2004) Mechanical assemblies. Oxford University Press, Oxford
23. Ding Y, Ceglarek D, Shi J (2000) Modeling and diagnosis of multistage manufacturing process: part I—state space model. In: Japan/USA symposium on flexible automation, Ann Arbor, MI
24. Li EE, Zhang HC (2001) Theoretical tolerance stackup analysis based on tolerance zone analysis. Int J Adv Manuf Technol 17:257–262
25. Pitman J (1993) Probability. Springer, New York